AePW-4 High-Angle Working Group Meeting

September 12, 2024

Pawel Chwalowski
Pawel.Chwalowski@nasa.gov

Agenda, September 12

- October/November DPW8-AePW4 joint meeting
- AIAA SciTech 2025: Orlando, FL
- Spring/Summer 2025: New BSCW Experiment
- Two presentations today:
  - Aerodynamic autoregressive model, Ron Efrati, Prof. Daniella Raveh, Technion
  - ROM Analysis, Prof. Marcello Righi, Zurich University of Applied Sciences

- Next meeting, October 10.

Schedule/Timeline/Logistics

- Monthly meetings on second Thursday of each month at 10 am EDT
- AIAA Aviation 2024: Las Vegas, NV - Bret Stanford
- AIAA SciTech 2025: Orlando, FL (?)
- Spring 2025: New BSCW Experiment (Data release ?)
-
- AIAA Aviation 2026: DPW-8 and AePW-4 Workshop

AePW-4 High-Angle WG Cases

- Mandatory
  - Flutter prediction at Mach 0.80 and angle-of-attack sweep: 0° – 6°
- Optional
  - Flutter prediction at Mach 0.78, 0.76, 0.74 and angle-of-attack 3°

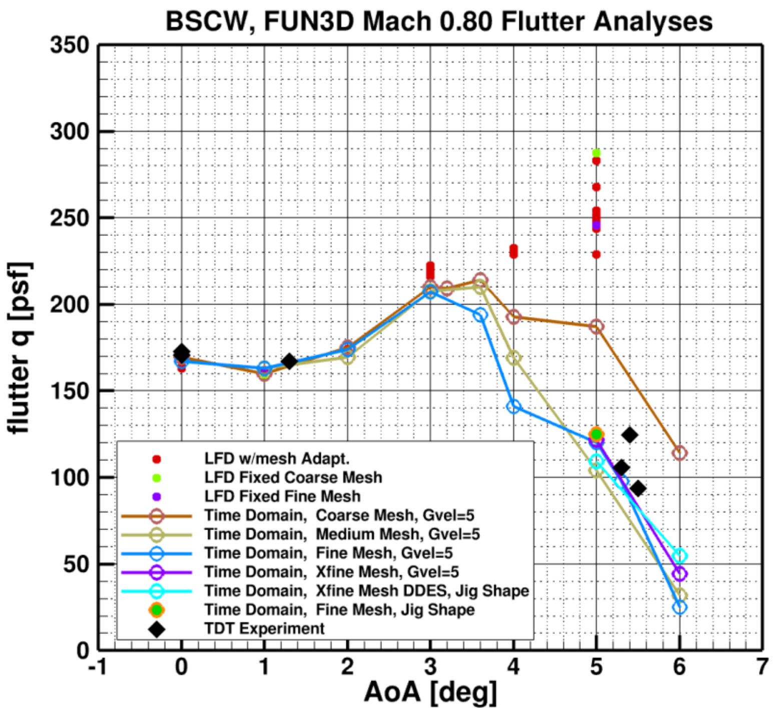

BSCW Experimental Data, Upper Surface

Shock-Buffet Prediction Report in Support of the
High Angle Working Group at the
Third Aeroelastic Prediction Workshop
https://doi.org/10.2514/6.2024-0417, Figure 3b

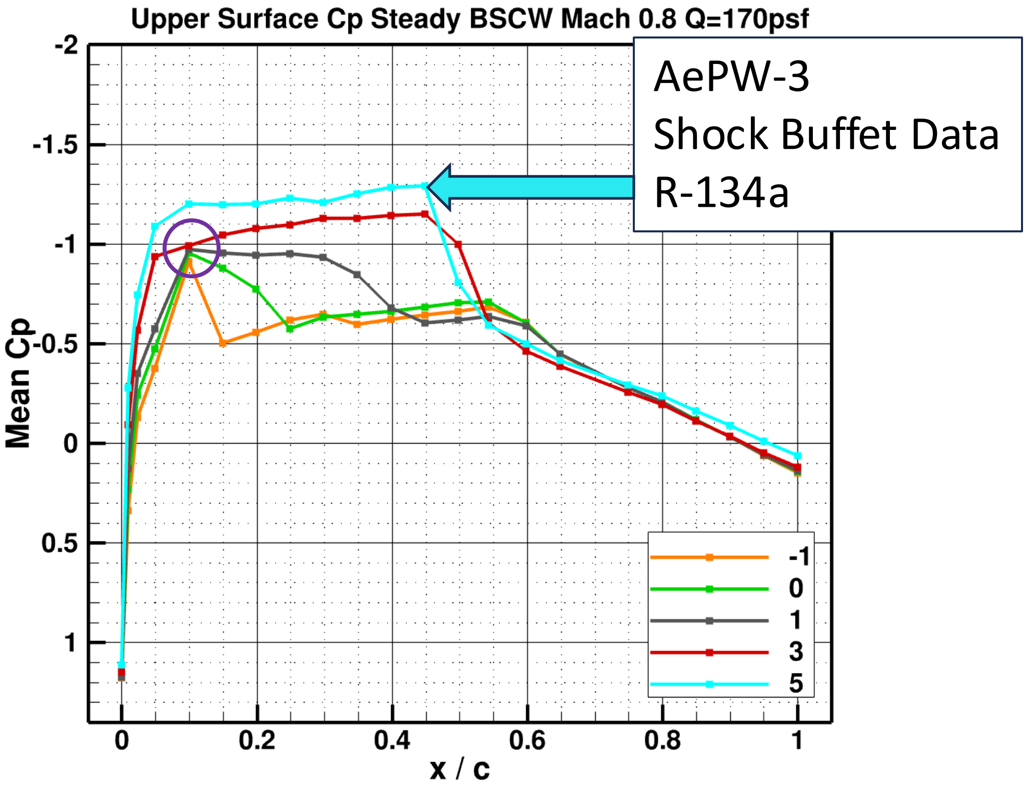

Rigidized OTT !!!

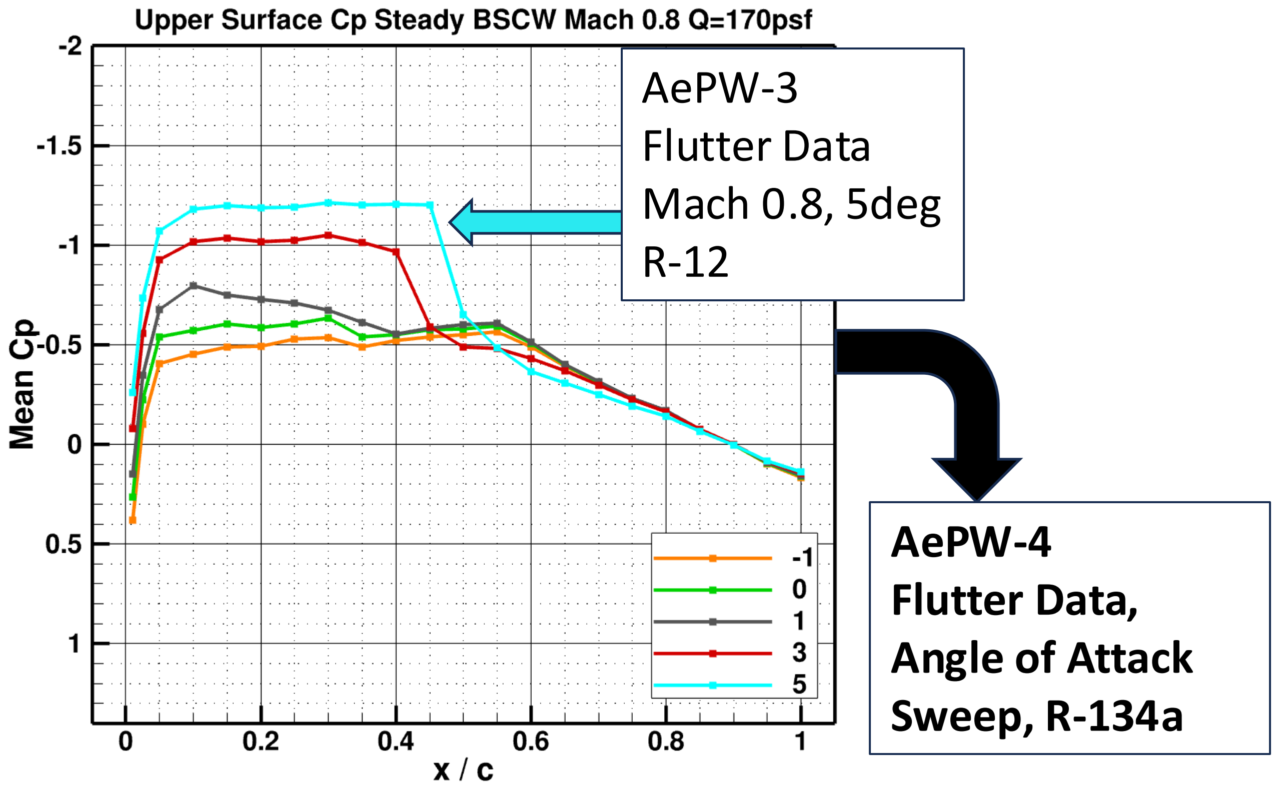

Rigidized PAPA !!!

BSCW Experimental Data, Lower Surface

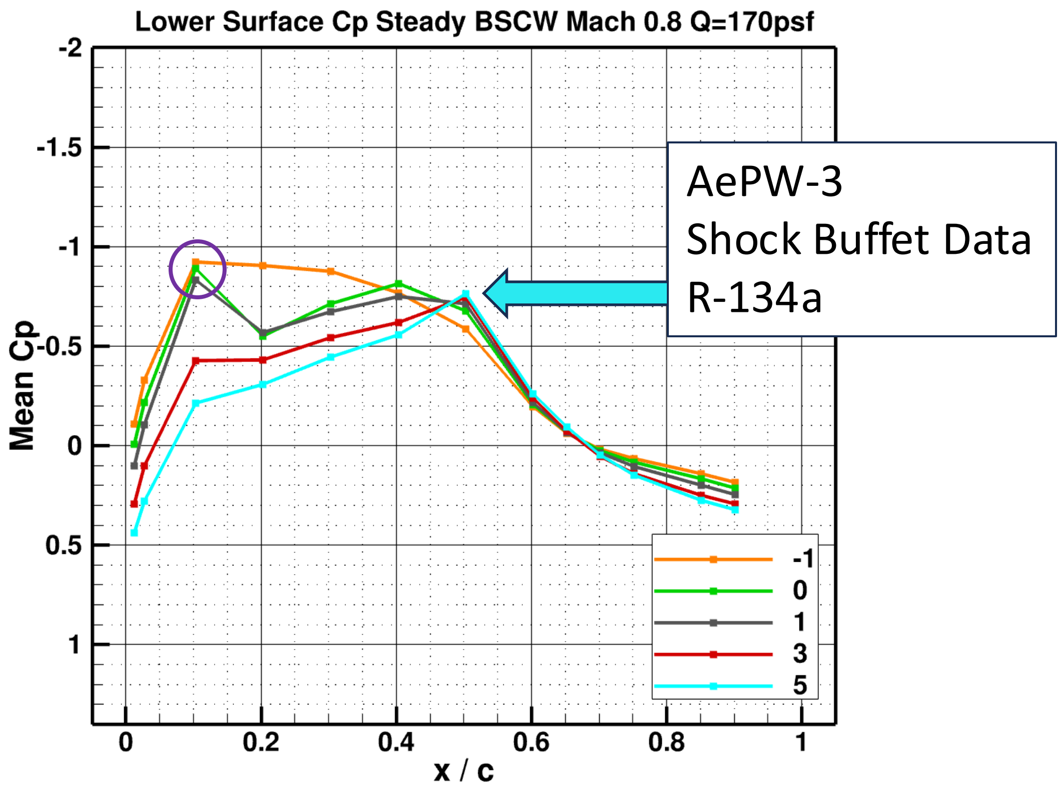

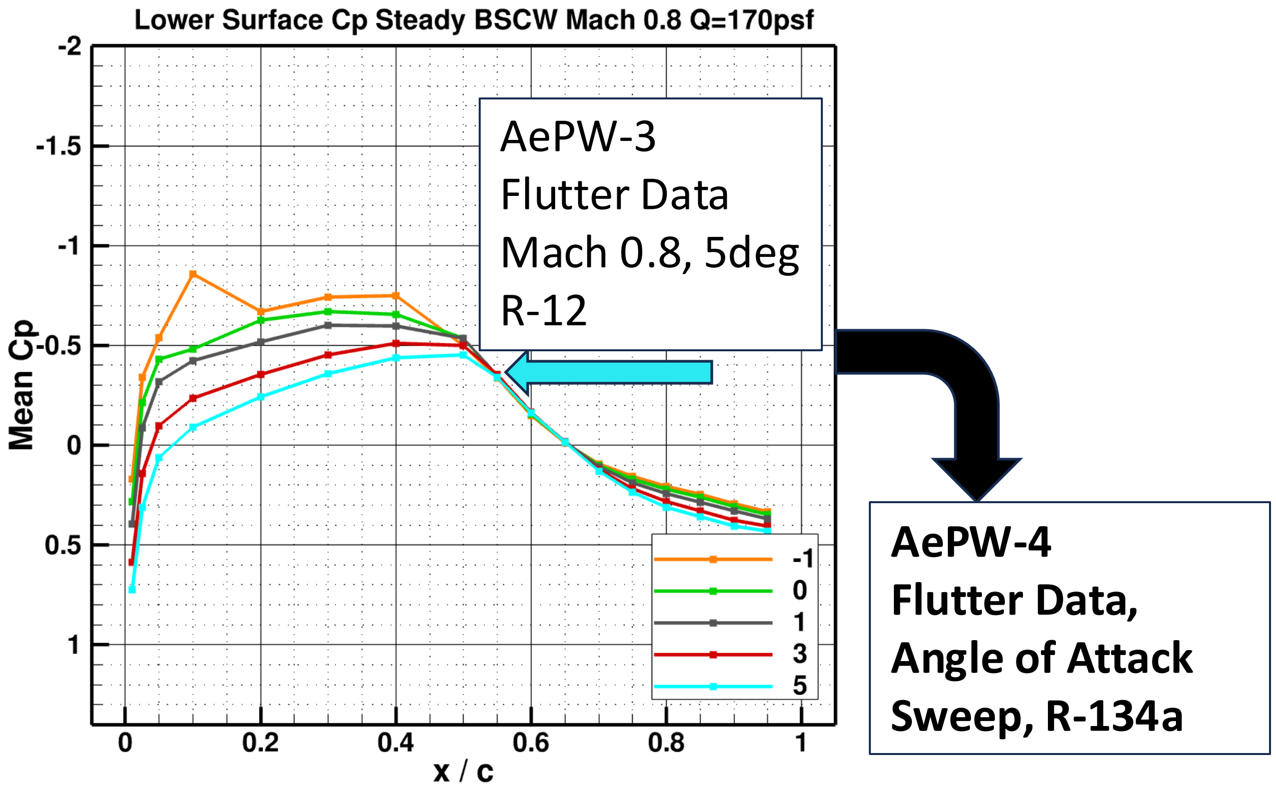

Rigidized OTT !!!

Rigidized PAPA !!!

PAPA vs. OTT vs. TAU vs. FUN3D (steady, upper surface)

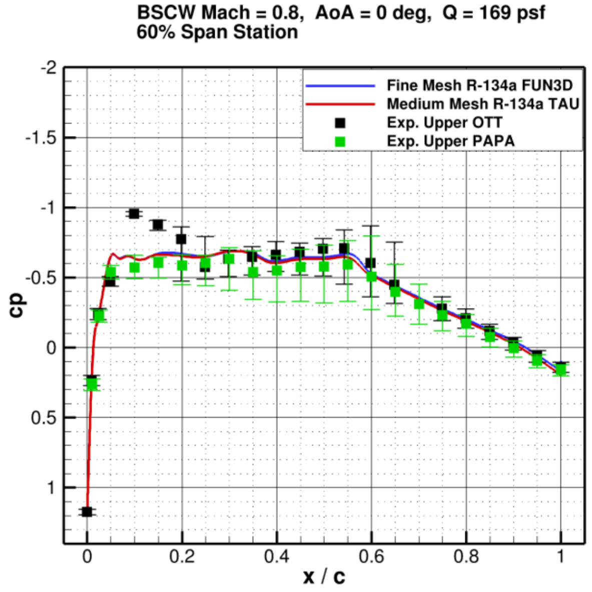

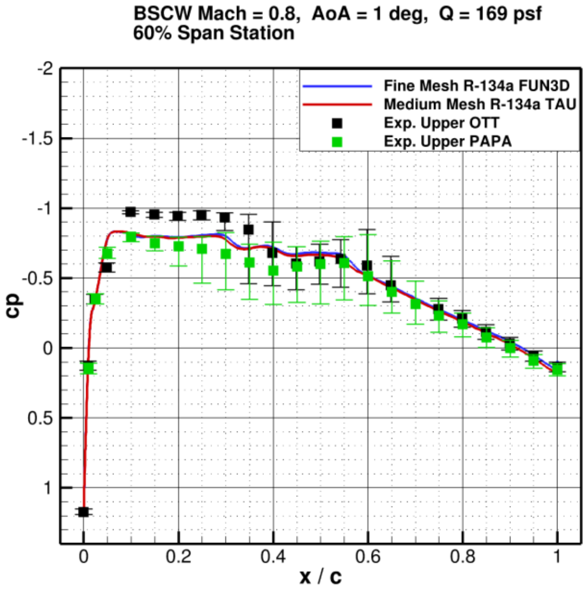

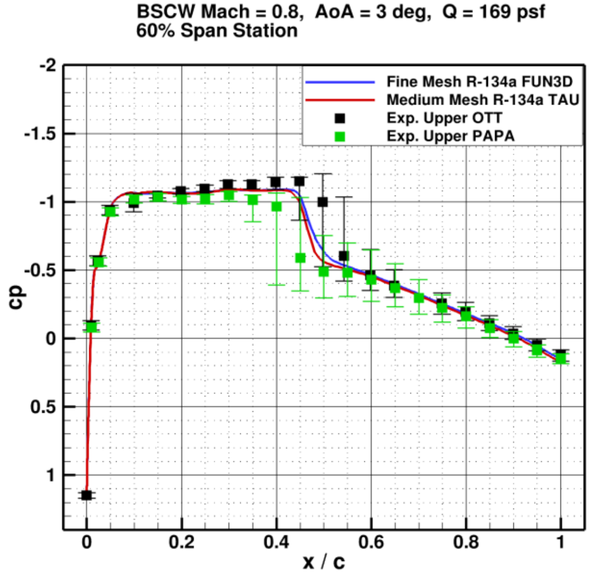

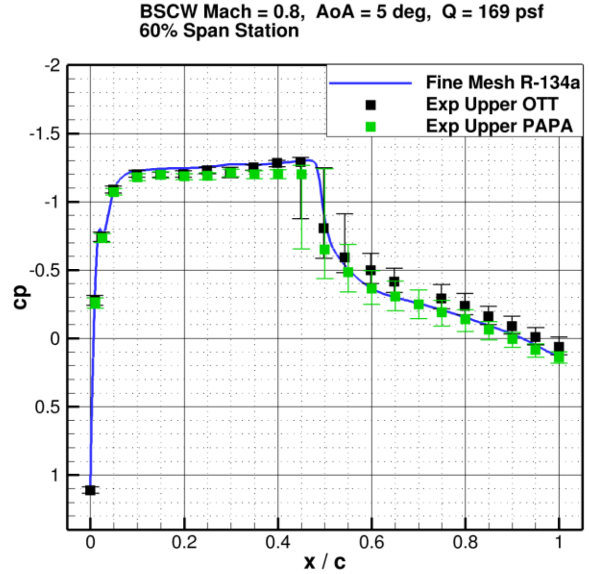

PAPA vs. OTT vs. TAU vs. FUN3D (steady, lower surface)

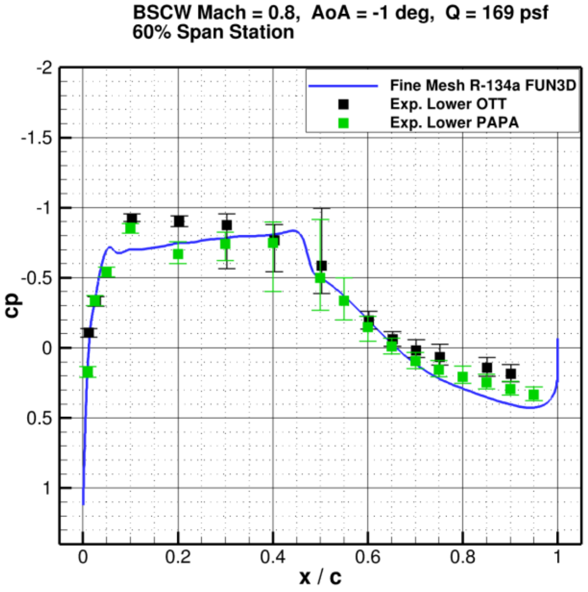

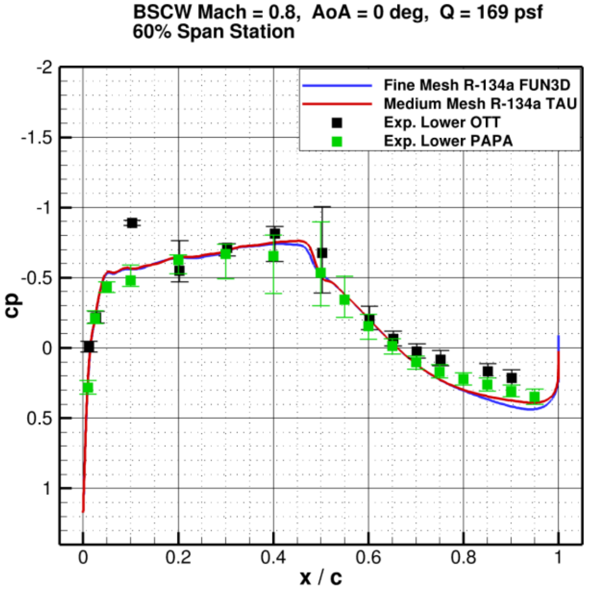

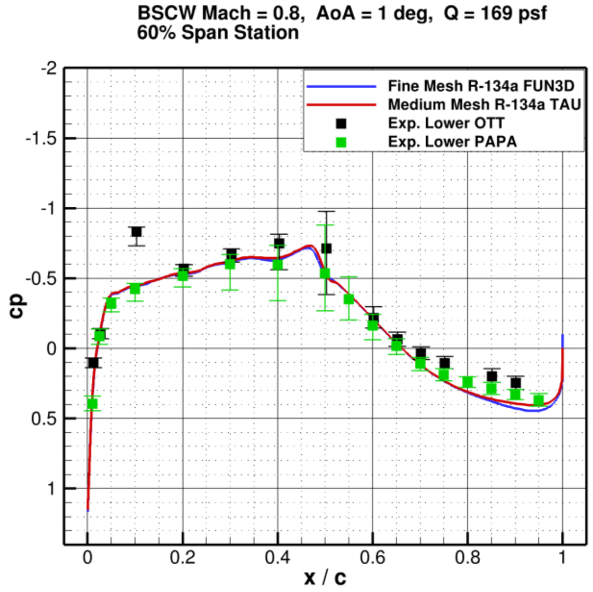

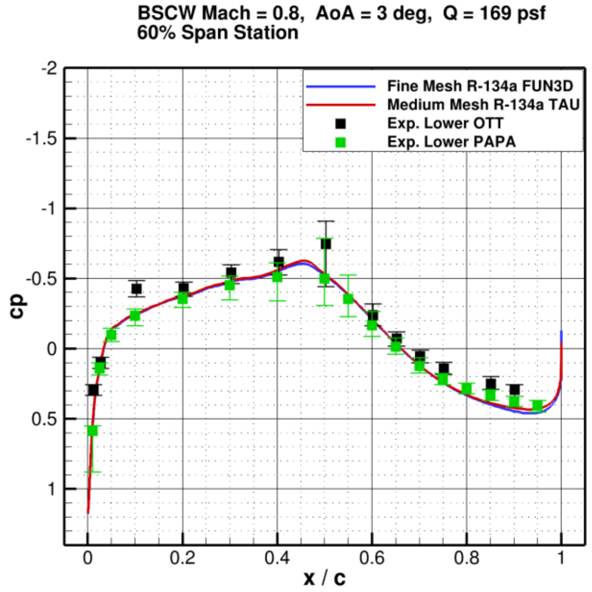

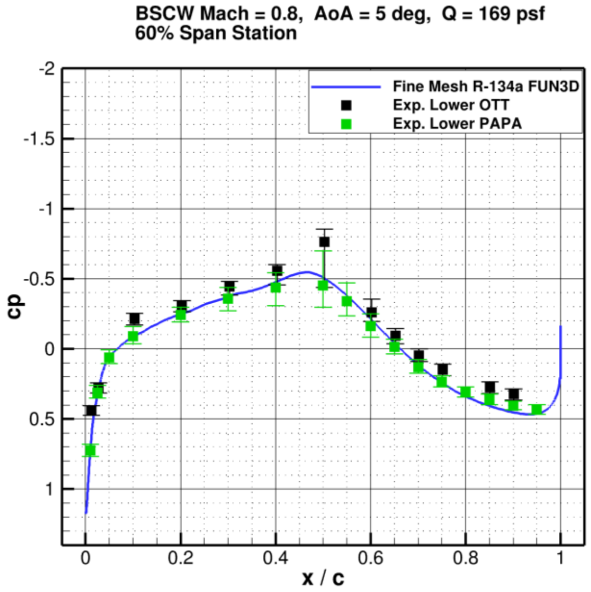

Dansberry Paper, AIAA93-1592, BSCW PAPA flutter

In air the boundaries were defined with and without fixed boundary layer transition. To fix the transition point a grit strip, 0.25" in width, running from root to tip on both the upper **and** lower surfaces was used. Two fixed transition configurations and one free transition configuration were tested in air. In R-12 only one configuration was tested. It had fixed transition.

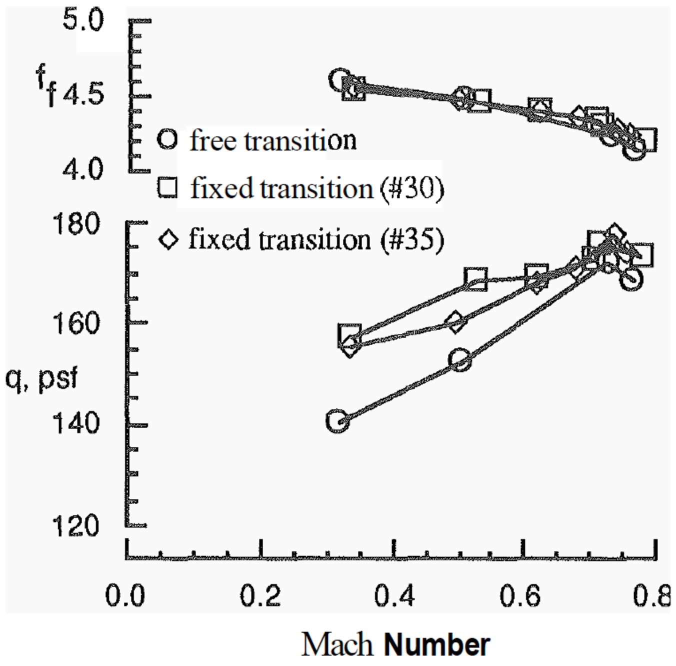

Figure 6. Transition effects on conventional flutter boundary in air (α_m=0°).

Figure 6 shows the effects on the flutter boundary in air of fixing the point on the model where the boundary layer transitions from laminar to turbulent. As mentioned previously, two different fixed transition configurations were tested. In both cases the transition point was fixed at 6.5 percent chord on both the upper and lower surfaces. The difference in the two configurations was a change in grit size from #30 to #35. Also, the transition strip used for the #35 grit configuration was wrapped around the tip while the #30 configuration left transition free on the tip. As can be seen in the figure, the main effect of fixing the transition point was to increase the flutter dynamic pressure. This effect is greater at subsonic Mach numbers than at transonic Mach numbers. The two transition fixed configurations show no significant differences.

All rigidized data were acquired using the #35 grit fixed transition configuration.

Piatak Paper, AIAA2002-0171: BSCW OTT

Boundary-layer transition was fixed at 7.5 percent chord using a #30 grit strip.

Conclusions

- Mandatory
  - Flutter prediction at Mach 0.80 and angle-of-attack sweep: 0° – 6°
- Optional
  - Flutter prediction at Mach 0.78, 0.76, 0.74 and angle-of-attack 3°

- **We use PAPA data (rigidized and flutter) for AePW-4 !!!**
- **Next BSCW experimental data (spring/summer 2025) must match existing PAPA data.**

CAD, Grids, Computational domain, Flow conditions,….

AePW-3 Summary Paper, https://doi.org/10.2514/6.2024-0418

Table 2 BSCW flow conditions: Mach 0.8 with range of dynamic pressure (q); chord Reynolds number (Re_c); Reynolds number per foot (Re); velocity (V); speed of sound (a); static temperature, (T_{static}); density (ρ); ratio of specific heat (γ); viscosity (μ); Prandtl number (Pr); total pressure (H); and static pressure (P).

Mach	0.799	0.8	0.8	0.8	0.8	0.8	0.8	0.8	0.8	0.8	0.8	0.801	0.801
q [psf]	10.02	25.00	35.00	50.00	75.00	100.00	134.00	143.00	152.00	168.80	200.00	225.00	250.00
Re_c	237461	592224	829213	1184801	1777732	2371336	3178880	3392751	3606668	4006103	4748658	5343835	5939368
Re [1/ft]	178096	444168	621910	888601	1333299	1778502	2384160	2544563	2705001	3004577	3561493	4007876	4454526
V [ft/s]	440.45	440.63	440.59	440.51	440.39	440.21	440.05	440.00	439.96	439.88	439.70	439.58	439.46
a [ft/s]	551.08	550.94	550.85	550.71	550.48	550.25	549.94	549.86	549.78	549.62	549.34	549.11	548.88
T_{static} [$^\circ F$]	80.87	80.83	80.83	80.82	80.81	80.80	80.78	80.77	80.77	80.76	80.74	80.73	80.71
ρ [slug/ft^3]	0.000103	0.000258	0.000361	0.000515	0.000774	0.001032	0.001384	0.001477	0.001571	0.001745	0.002069	0.002329	0.002589
γ	1.1121	1.1122	1.1123	1.1124	1.1126	1.1128	1.1131	1.1131	1.1132	1.1133	1.1136	1.1138	1.1139
μ [lb-sec/ft^2]	2.555e-07	2.555e-07	2.555e-07	2.555e-07	2.555e-07	2.555e-07	2.554e-07	2.554e-07	2.554e-07	2.554e-07	2.554e-07	2.554e-07	2.554e-07
Pr	0.68394	0.68404	0.68410	0.68419	0.68435	0.68450	0.68471	0.68477	0.68483	0.68493	0.68513	0.68528	0.68544
H [psf]	40.00	99.72	139.61	199.45	299.18	399.00	534.69	570.61	606.53	673.59	798.21	898.01	997.83
P [psf]	28.21	70.32	98.45	140.64	210.97	281.37	377.05	402.38	427.71	475.00	562.87	633.25	703.64

CAD, Grids, Computational domain, Flow conditions,….

Mach 0.74

Mach	0.74	0.74	0.74	0.74	0.74	0.74	0.74	0.74
q [psf]	50.00	75.00	100.00	134.00	143.00	152.00	168.80	200.00
Re_c	1275964	1914959	2554246	3423935	3654400	3884927	4315413	5115471
Re [1/ft]	956973	1436219	1915684	2567951	2740800	2913695	3236560	3836603
V [ft/s]	407.58	407.37	407.23	407.09	407.04	406.99	406.89	406.71
a [ft/s]	550.82	550.56	550.30	549.93	549.84	549.74	549.56	549.23
T_{static} [$^\circ F$]	83.60	83.59	83.58	83.55	83.55	83.54	83.54	83.52
ρ [slug/ft^3]	0.000602	0.000904	0.001206	0.001617	0.001726	0.001836	0.002039	0.002418
γ	1.1116	1.1119	1.1121	1.1124	1.1125	1.1125	1.1127	1.1130
μ [lb-sec/ft^2]	2.564E-07	2.564E-07	2.564E-07	2.564E-07	2.564E-07	2.564E-07	2.564E-07	2.563E-07
Pr	0.68325	0.68343	0.68360	0.68385	0.68391	0.68398	0.68410	0.68432
H [psf]	221.92	332.99	444.03	594.95	634.93	674.92	749.56	888.22
P [psf]	164.50	246.83	329.14	441.01	470.65	500.29	555.62	658.40

CAD, Grids, Computational domain, Flow conditions,....

Mach 0.76

Mach	0.76	0.76	0.76	0.76	0.76	0.76	0.76	0.76
q [psf]	50.00	75.00	100.00	134.00	143.00	152.00	168.80	200.00
Re_c	1245425	1868520	2492233	3341185	3566044	3790959	4210646	4991103
Re [1/ft]	934069	1401390	1869175	2505889	2674533	2843219	3157984	3743327
V [ft/s]	418.22	418.15	418.01	417.82	417.78	417.73	417.67	417.50
a [ft/s]	550.43	550.18	549.93	549.58	549.49	549.40	549.23	548.92
T_{static} [$^\circ F$]	82.72	82.70	82.69	82.67	82.67	82.66	82.65	82.63
ρ [slug/ft^3]	0.000572	0.000858	0.001145	0.001535	0.001639	0.001742	0.001936	0.002295
γ	1.1118	1.1120	1.1122	1.1125	1.1125	1.1126	1.1128	1.1130
μ [lb-sec/ft^2]	2.560E-07	2.560E-07	2.560E-07	2.560E-07	2.560E-07	2.560E-07	2.560E-07	2.559E-07
Pr	0.68360	0.68377	0.68394	0.68417	0.68423	0.68430	0.68441	0.68463
H [psf]	213.86	320.74	427.68	573.16	611.67	650.19	722.01	855.54
P [psf]	155.96	233.91	311.91	418.00	446.09	474.18	526.56	623.94

CAD, Grids, Computational domain, Flow conditions,….

Mach 0.78

Mach	0.78	0.78	0.78	0.78	0.78	0.78	0.78	0.78
q [psf]	50.00	75.00	100.00	134.00	143.00	152.00	168.80	200.00
Re_C	1216355	1824869	2433950	3262935	3482495	3702106	4112185	4874236
Re [1/ft]	912266	1368652	1825462	2447201	2611871	2776579	3084139	3655677
V [ft/s]	428.90	428.83	428.70	428.53	428.48	428.43	428.35	428.19
a [ft/s]	550.03	549.79	549.55	549.22	549.13	549.05	548.88	548.58
T_{static} [$^\circ F$]	81.82	81.80	81.79	81.77	81.76	81.76	81.75	81.73
ρ [slug/ft^3]	0.000544	0.000816	0.001088	0.001460	0.001558	0.001656	0.001840	0.002182
γ	1.1119	1.1121	1.1123	1.1125	1.1126	1.1127	1.1128	1.1131
μ [lb-sec/ft^2]	2.556E-07	2.556E-07	2.556E-07	2.556E-07	2.556E-07	2.556E-07	2.555E-07	2.555E-07
Pr	0.68396	0.68413	0.68429	0.68451	0.68457	0.68463	0.68474	0.68495
H [psf]	206.41	309.56	412.78	553.16	590.33	627.50	696.88	825.74
P [psf]	148.06	222.05	296.08	396.78	423.44	450.10	499.87	592.30

AePW-4 High-Angle Working Group Meeting

June 13, 2024

Pawel Chwalowski
Pawel.Chwalowski@nasa.gov